ISSN 1070-3284, Russian Journal of Coordination Chemistry, 2017, Vol. 43, No. 12, pp. 843–851. © Pleiades Publishing, Ltd., 2017.
Original Russian Text © A.I. Poddel'sky, M.V. Arsen'ev, L.S. Okhlopkova, I.V. Smolyaninov, G.K. Fukin, 2017, published in Koordinatsionnaya Khimiya, 2017, Vol. 43, No. 12, pp. 744–753.

New Catecholate Complexes of Triphenylantimony(V) Based on 6-Iminomethyl-3,5-Di-*tert*-Butylpyrocatechols N-Functionalized by the Aniline or Phenol Group

A. I. Poddel'sky[a], *, M. V. Arsen'ev[a], L. S. Okhlopkova[a], I. V. Smolyaninov[b, c], and G. K. Fukin[a]

[a] *Razuvaev Institute of Organometallic Chemistry, Russian Academy of Sciences, ul. Tropinina 49, Nizhny Novgorod, 603600 Russia*

[b] *Astrakhan State Technical University, Astrakhan, Russia*

[c] *Southern Scientific Center, Russian Academy of Sciences, Rostov-on-Don, Russia*

**e-mail: aip@iomc.ras.ru*

Received June 28, 2017

Abstract—The following new triphenylantimony(V) catecholate complexes bearing the protonated imine group are synthesized from the new sterically hindered 3,5-di-*tert*-butylpyrocatechols (6-(CH=N-*o*-(C_6H_4–NH_2))-3,5-Cat)H_2 (H_2L^1) and (6-(CH=N-*o*-(C_6H_4–OH))-3,5-Cat)H_2 (H_2L^2) containing in position 6 the iminomethyl group bonded to the aniline or phenol substituent: (6-(CH=NH^+-*o*-(C_6H_4–NH_2))-3,5-Cat)$SbPh_3X$ (X = Br (**I**), OMe (**III**)) and (6-(CH=NH^+-*o*-(C_6H_4–OH))-3,5-Cat)$SbPh_3X$ (X = Br (**II**), OMe (**IV**)). The molecular structure of complex **III** · CH_3OH in the crystalline state is determined by X-ray diffraction analysis (CIF file CCDC no. 1554694). The electrochemical properties of complexes **III** and **IV** are studied by cyclic voltammetry.

Keywords: redox-active ligand, antimony, pyrocatechol, quinone, X-ray diffraction analysis, cyclic voltammetry

DOI: 10.1134/S1070328417120089

INTRODUCTION

Antimony and its compounds find use in various areas of fundamental and applied science [1–5]. The coordination antimony compounds with redox-active ligands of the *o*-quinone type are interesting for researchers from the viewpoint of both diversity of structural types formed by them [6–8] and specific features of the chemical behavior demonstrated by this class of compounds [9–13]. The triphenylantimony(V) complexes with catecholate and *o*-amidophenolate ligands are the first examples for coordination compounds of non-transition metals capable of reversible binding molecular oxygen [13–15]. The studies of this class of compounds show that the nature of substituents in the redox-active ligand exerts a substantial effect on both the redox properties of the catecholate complexes [16–19] and their chemical behavior and biochemical activity [20–26]. The functionalization of 3,5-di-*tert*-butylpyrocatechol (*o*-quinone) to position 6 by the aldehyde or substituted iminomethyl group makes it possible to obtain new polyfunctional redox-active ligands in which this additional group acts as both the modulator of redox properties and active participant of chemical processes [27–29]. For example, 3,5-di-*tert*-butylpyrocatechol containing ferrocene bound to the aromatic ring of pyrocatechol in position 6 by the 1,2-dimethylenehydrazine bridge (–CH=N–N=CH–) in the reaction with tin and antimony organohalides gives not classical catecholates formed by the complete substitution of the hydrogen atoms of the hydroxy groups by the metal atom but the stable zwitterionic derivatives bearing the hydraziniumylidene cation (–CH=NH^+–N=CH–) and complex metal-containing anion (Scheme 1) [29]. These structures can be formed due to the formation of a six-membered ring with the stable intramolecular hydrogen bond between the NH^+ fragment and oxygen atom of the catecholate ligand (Scheme 1).

In this work, we describe the new triphenylantimony complexes based on the redox-active ligands of the *o*-quinone type containing the aniline or phenol functions bound to the *o*-quinone framework in position 6 by the imine group (–CH=N–).

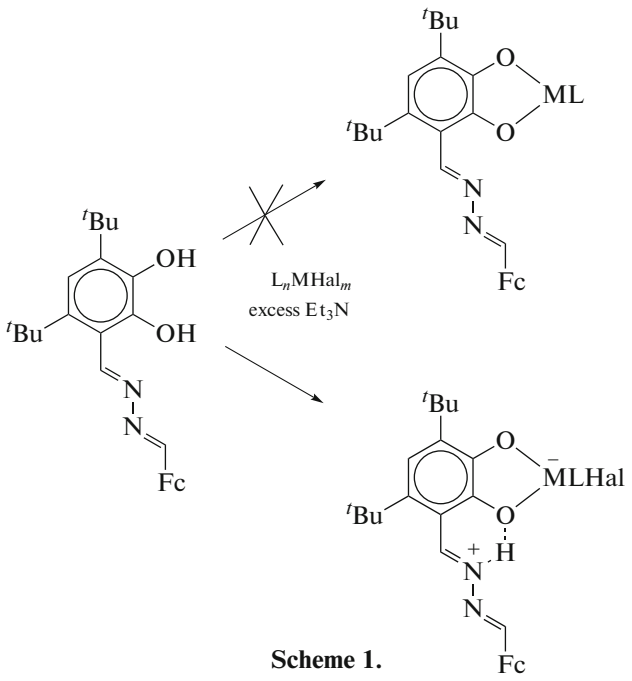

Scheme 1.

EXPERIMENTAL

The used solvents were purified and dehydrated using standard procedures [30]. 6-(2-Aminophenyliminomethyl)-3,5-di-*tert*-butylpyrocatechol, (6-(CH=N-*o*-(C_6H_4–NH_2))-3,5-Cat)H_2 (H_2L^1), was synthesized using a known procedure [31], and 6-formyl-3,5-di-*tert*-butylpyrocatechol was synthesized according to [27]. The complexes were synthesized in evacuated ampules in the absence of oxygen.

Synthesis of 6-(2-hydroxyphenyliminomethyl)-3,5-di-*tert*-butylpyrocatechol (6-(CH=N-*o*-(C_6H_4–OH))-3,5-Cat)H_2 (H_2L^2). 6-Formyl-3,5-di-*tert*-butylpyrocatechol (2 g, 8 mmol) was added with stirring to a solution of *o*-aminophenol (0.856 g, 8 mmol) in MeOH (20 mL). The mixture was refluxed for 2 h. Then the reaction mixture was cooled to room temperature. The product was filtered off, washed with cold methanol, dried in vacuo, and isolated as bright red finely crystalline powder (2.37 g, 87%).

For $C_{21}H_{27}N_1O_3$

Anal. calcd., %	C, 73.87	H, 7.97	N, 4.10
Found, %	C, 73.93	H, 7.95	N, 4.05

^{1}H NMR (δ, ppm): 1.44 s (9H, ^{t}Bu), 1.50 s (9H, ^{t}Bu), 6.0–6.7 br.s (1H, OH), 6.83 s (1H, C_6H_1), 6.92–7.07 m (2H, Ar), 7.10–7.24 m (2H, Ar).

Synthesis of (6-(CH=NH^+-*o*-(C_6H_4–NH_2))-3,5-Cat)$SbPh_3Br$ (I). A solution of substituted pyrocatechol H_2L^1 (171 mg, 0.5 mmol) in toluene (20 mL) was added with stirring to a solution of triphenylantimony dibromide (256 mg, 0.5 mmol) in toluene (20 mL). After H_2L^1 was completely added, the solution was stirred with slight heating for 30 min, and triethylamine (0.28 mL, 2 mmol) in toluene (15 mL) was added continying stirring. The solution gained dark cherry color, and the formation of a weakly colored precipitate was observed. The reaction mixture was stirred on heating for 1 h, after which a precipitate of triethylammonium bromide was filtered under reduced pressure. Toluene was replaced by hexane, and the obtained solution was left to stay for 2 days at –12°C. The formed powdered dark cherry precipitate of complex **I** was filtered off and dried in vacuo. The yield of compound **I** was 250 mg (64.7%).

For $C_{39}H_{42}N_2O_2BrSb$

Anal. calcd., %	C, 60.64	H, 5.48	Sb, 15.76	Br, 10.34
Found, %	C, 60.22	H, 5.30	Sb, 16.01	Br, 10.50

^{1}H NMR (δ, ppm): 1.44 s (9H, ^{t}Bu), 1.49 s (9H, ^{t}Bu), 3.10 br.s (2H, NH_2), 6.76 s (1H, C_6H_1), 6.8–7.3 m (11H, Ar), 7.4–7.7 m (8H, Ar), 9.10 s (1H, CH=N), 11.50 br.s (1H, NH).

Synthesis of (6-(CH=NH^+-*o*-(C_6H_4–OH))-3,5-Cat)$SbPh_3Br$ (II). Complex **II** was synthesized similarly to the synthesis of compound **I** from triphenylantimony dibromide (256 mg, 0.5 mmol) and pyrocatechol H_2L^2. The yield of powdered compound **II** was 225 mg (58.2%).

For $C_{39}H_{41}NO_3BrSb$

Anal. calcd., %	C, 60.57	H, 5.34	Sb, 15.74	Br, 10.33
Found, %	C, 60.09	H, 5.10	Sb, 16.10	Br, 10.56

^{1}H NMR (δ, ppm): 1.26 s (9H, ^{t}Bu), 1.35 s (9H, ^{t}Bu), 6.68 s (1H, C_6H_1), 6.9–7.2 m (12H, Ar), 7.3–7.5 m (9H, Ar, OH), 9.07 s (1H, CH=N), 10.88 br.s (1H, NH).

Synthesis of (6-(CH=NH^+-*o*-(C_6H_4–NH_2))-3,5-Cat)$SbPh_3(OMe)\cdot CH_3OH$ (III · CH_3OH). A weighed sample of complex **I** (180 mg, 0.23 mmol) was dissolved in methanol (25 mL), and triethylamine (0.07 mL, 0.5 mmol) was added to the solution. The reaction mixture was stirred on heating for 2 h and concentrated under reduced pressure by ~2 times. The obtained solution was left to stay for 24 h at –12°C. The formed finely crystalline dark cherry powder of complex **III · CH_3OH** was filtered off and dried in vacuo. The yield was 120 mg (68.1%).

For $C_{41}H_{49}N_2O_4Sb$

Anal. calcd., %	C, 65.17	H, 6.54	Sb, 16.11
Found, %	C, 64.87	H, 6.20	Sb, 16.48

^{1}H NMR (δ, ppm): 1.46 s (18H, ^{t}Bu), 2.67 br.s (2H, NH_2), 3.44 s (CH_3, MeO), 3.46 s (CH_3, MeOH), 6.80 s (1H, C_6H_1), 6.6–6.9 m (5 H, Ar), 7.08 m (2H,

Ar), 7.2–7.5 m (8H, Ar), 7.5–7.6 m (1H, Ar), 7.65–7.85 m (4H, Ar), 9.12 s (1H, CH=N), 14.00 br.s (1H, NH).

A sample of complex **III** containing no crystallization molecule of methanol was obtained by recrystallization from toluene.

Synthesis of (6-(CH=NH$^+$-*o*-(C_6H_4–OH))-3,5-Cat)$SbPh_3$(OMe) · CH_3OH (IV · CH_3OH). A sample of complex **IV · CH_3OH** was synthesized similarly to the synthesis of compound **III · CH_3OH** from complex **II** in methanol. The yield of the product was 130 mg (73.8%).

For $C_{41}H_{48}NO_5Sb$			
Anal. calcd., %	C, 65.09	H, 6.39	Sb, 16.09
Found, %	C, 64.87	H, 6.20	Sb, 16.48

^{1}H NMR (δ, ppm): 1.01 s (9H, ^{t}Bu), 1.54 s (9H, ^{t}Bu), 3.48 s (CH_3, MeO), 3.51 s (CH_3, MeOH), 6.70 s (1H, C_6H_1), 6.6–7.0 m (4 H, Ar), 7.3–7.5 m (10H, Ar), 7.7–7.8 m (6H, Ar), 9.75 br.s (1H, CH=N), 13.74 br.s. (1H, NH).

A sample of complex **IV** containing no crystallization molecule of methanol was obtained by recrystallization from toluene.

^{1}H NMR spectra were recorded on a Bruker AVANCE DPX-200 spectrometer using tetramethylsilane as an internal standard and $CDCl_3$ as a solvent.

The electrochemical potentials of the studied compounds were measured by cyclic voltammetry (CV) in a three-electrode cell with an IPC-pro potentiostat in dichloromethane or acetonitrile under an argon atmosphere. The working electrode was a stationary glassy carbon (GC) electrode with a diameter of 2 mm, and a platinum plate (S = 18 mm^2) served as the auxiliary electrode. The used reference electrode (Ag/AgCl/KCl) had a water-impervious membrane. The concentration of compounds **III** and **IV** was 0.0005–0.003 mol/L. The number of electrons transferred in the course of the electrode process was estimated relative to ferrocene used as a standard. The potential sweep was 0.2 V s^{-1}, and the supporting electrolyte was 0.1 M Bu_4NClO_4 (99%, Acros).

The X-ray diffraction analysis of complex **III · CH_3OH** was carried out on a Bruker D8 Quest CMOS diffractometer at 100 K. The structure was solved by a direct method and refined by full-matrix least squares for F^2_{hkl} in the abisotropic approximation for all non-hydrogen atoms. Hydrogen atoms were placed in the geometrically calculated positions and refined isotropically. The calculations were performed using the SHELXTL program package [32]. An absorption correction was applied using the SADABS program [33]. The crystallographic data and the X-ray diffraction experimental and structure refinement parameters for compound **III · CH_3OH** are presented in Table 1. The structural data for **III · CH_3OH** were deposited with the Cambridge Crystallographic Data Centre (CIF file CCDC no. 1554694; deposit@ccdc.cam.ac.uk; www: http://www.ccdc.cam.ac.uk).

RESULTS AND DISCUSSION

The exchange reactions of pyrocatechols H_2L^1 and H_2L^2 with triphenylantimony dibromide in the presence of an insignificant triethylamine excess in a toluene solution (Scheme 2) was found to lead to the deprotonation of only one hydroxyl group of pyrocatechol and to the formation of partially substituted derivatives **I** and **II** in which the bromide atom at the central antimony atom is retained and the proton from the hydroxyl group in the position adjacent to the iminomethyl group migrates to the nitrogen atom to form the iminium cation. The formation of similar structures was shown for the tin(IV) and antimony(V) catecholate complexes containing the –CH=N–N=CH–Fc group (Fc is ferrocenyl) in position 6 of the 3,5-di-*tert*-butylcatecholate ligand [29].

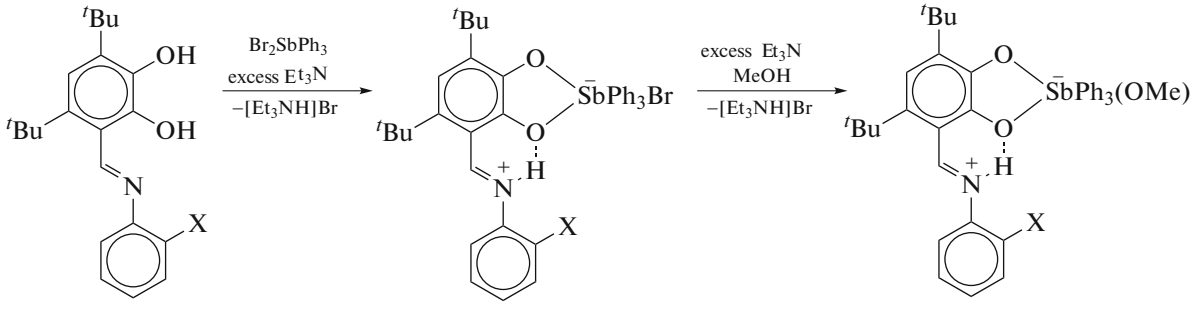

X = NH_2 (H_2L^1) **I**
OH (H_2L^2) **II**
III
IV

The treatment of complexes **I** and **II** with a triethylamine excess in a methanol solution even on heating did not result in the deprotonation of the nitrogen atom and formation of "classical" triphenylantimony(V) catecholate in which catecholate acts as a dianionic ligand. The methanol molecule was deprotonated instead of the

Table 1. Crystallographic data and the X-ray diffraction experimental and structure refinement parameters for compound **III · CH_3OH**

Parameter	Value
Empirical formula	$C_{41}H_{49}N_2O_4Sb$
FW	755.57
T, K	100(2)
Wavelength, Å	0.71073
Crystal system	Orthorhombic
Space group	*Pbca*
Crystal cell parameters:	
a, Å	19.2459(9)
b, Å	18.9280(9)
c, Å	19.8041(9)
V, Å^3	7214.4(6)
Z	8
ρ_{calcd}, g/cm^3	1.391
μ, mm^{-1}	0.809
F(000)	3136
$2\theta_{max}$, deg	56
Number of measured reflections	59290
Number of independent reflections (R_{int})	8667 (0.0251)
Number of reflections with $I > 2\sigma(I)$	7703
Number of refined parameters	457
R_1, wR_2 ($I > 2\sigma(I)$)	0.0228, 0.0574
R_1, wR_2 (all reflections)	0.0277, 0.0591
Goodness-of-fit for F^2	1.045
Residual electron density (max/min), *e*/Å^3	0.617/–0.239

above expected processes with the replacement of the bromine atom in the coordination sphere of the central antimony atom by the methoxy group to form new complexes **III** and **IV**, respectively (Scheme 2). The complexes were isolated in the individual state as red-orange microcrystalline powders and characterized by the data of ^{1}H and ^{13}C NMR spectroscopy, IR spectroscopy, and elemental analysis.

The molecular structure of aniline-containing complex **III · CH_3OH** in the crystalline state was established by X-ray diffraction analysis (Fig. 1). Selected bond lengths and bond angles are given in Table 2.

The central Sb(1) atom in complex **III · CH_3OH** is in the distorted octahedral environment formed by the catecholate ligand, three phenyl groups, and methoxy substituent (Fig. 1). The equatorial plane is formed by the O(1) and O(2) oxygen atoms and C(28) and C(34) carbon atoms of two phenyl rings. The O(1)–C(1) and O(2)–C(2) bond lengths of the chelate-bound ligand lie in the range of ordinary O–C bonds (1.33–1.36 Å [7, 34–37]), which corresponds to the dianionic (catecholate) form of this ligand.

The Sb(1)–O(1) (2.1587(9) Å) and Sb(1)–O(2) (2.0532(10) Å) bond lengths correspond to the bond lengths in various antimony(V) catecholate complexes [38–40]. The Sb(1)–O(1) bond is somewhat longer than Sb(1)–O(2) due to the participation of the O(1) atom in the strong intramolecular hydrogen bond O(1)···H(1)–N(1) (O(1)···H(1) 1.882(18) Å, angle O(1)H(1)N(1) 138.4(16)°) with the formation of the almost planar six-membered cycle O(1)C(1)C(6)-C(15)N(1)H(1) (Fig. 2). The O(1)–C(1)–C(6)–C(15) torsion angle is 8.47°. The N(1)=C(15) group lies nearly in the plane of the six-membered carbon cycle C(1–6) of the catecholate ligand, whereas the aromatic ring of the aniline group shifts from this plane. The dihedral angle between the C(1–6) and C(16–21) planes is 18.61° (the C(15)–N(1)–C(16)–C(21) torsion angle is 18.97°). The Sb(1)–O(1S) distance is noticeably less (2.0381(10) Å) than the sum of covalent radii of Sb and O (2.16 Å [41]).

The crystals of compound **III · CH_3OH** contain intermolecular hydrogen bonds between the molecules of the complex and crystallization molecules of methanol. The latter is arranged in such a way that the O(2S) atom interacts with the H(3) atom of the amine group (O(2S)···H(3) (N(2)) 1.97(2) Å, angle O(2S)H(3)N(2) 169.2(18)°), and the H(2S) atom is

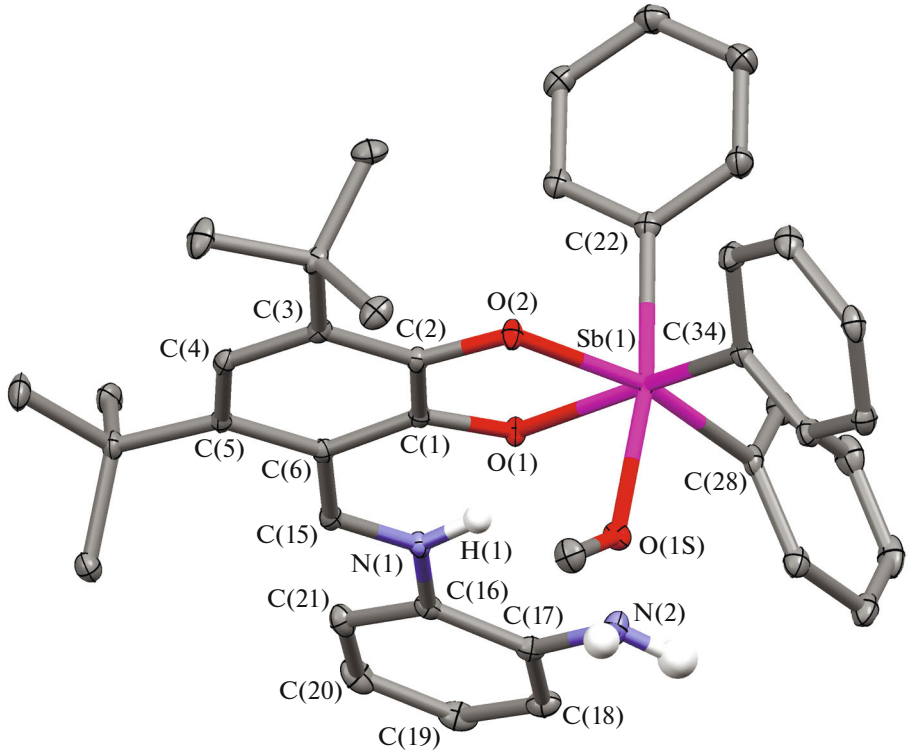

Fig. 1. Molecular structure of complex **III** · CH_3OH in the crystalline state according to the X-ray diffraction data. Hydrogen atoms, except for the hydrogen atoms at the nitrogen atoms, are omitted. Thermal ellipsoids are presented with 30% probability.

directed to the O(1S) atom of the methoxy group (O(1S)···H(2S)(O(2S)) 1.78(2) Å, angle O(1S)H(2S)-O(2S) 173(2)°) (Fig. 2).

The electrochemical properties of catecholate complexes **III** and **IV** were studied by the CV method in dichloromethane and acetonitrile at the GC electrode (Table 3). The studied complexes differ significantly in the redox behavior compared to the earlier considered triphenylantimony(V) catecholates, which are characterized by two oxidation steps corresponding to the formation of the mono- and dicationic complexes relatively stable in the time scale of the CV experiment [16–19]. For complex **IV** in the studied solvents, electrochemical oxidation is irreversible in the anodic range of potential sweep (Fig. 3).

The nature of the solvent used exerts no effect on the oxidation potentials, and the electrochemical parameters of the complex remain stable in time. The first irreversible anodic step presumably corresponds to the one-electron oxidation of the C–O group of catecholate bound to the adjacent iminomethyl group by the intramolecular hydrogen bond (Scheme 3). Irreversibility of the oxidation process indicates that the subsequent chemical step occurs: the proton is transferred to the iminomethyl group to form *o*-semiquinone coordinated to the antimony(V) atom. The second irreversible oxidation step characterizes the redox transition *o*-semiquinone/*o*-benzoquinone, and the value of the detected potential is well consistent with the earlier obtained data on the oxidation of the triphenylantimony(V) complexes bearing the catecholate ligands with the nitrogen-containing fragments [40].

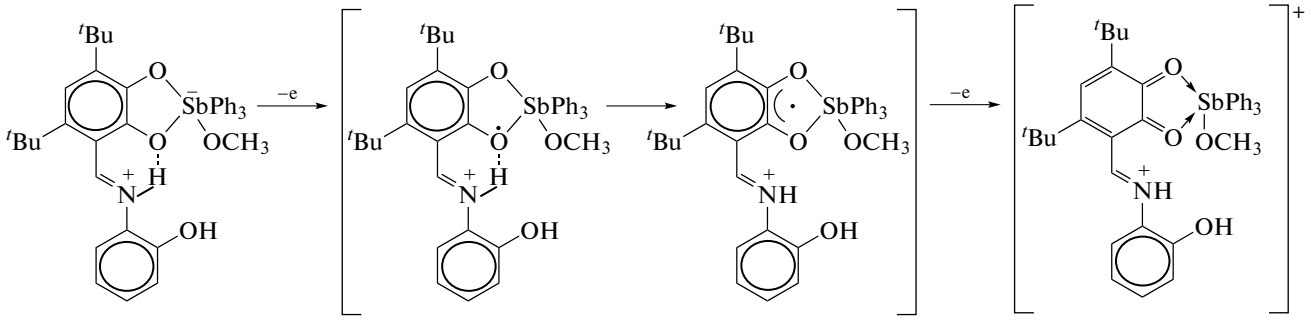

Scheme 3.

Table 2. Selected bond lengths (*d*) and bond angles (ω) in compound **III · CH_3OH**

Bond	*d*, Å
Sb(1)–O(1)	2.1587(9)
Sb(1)–O(2)	2.0532(10)
Sb(1)–O(1S)	2.0381(10)
Sb(1)–C(22)	2.1616(14)
Sb(1)–C(28)	2.1462(14)
Sb(1)–C(34)	2.1315(14)
O(1)–C(1)	1.3226(16)
O(2)–C(2)	1.3352(16)
N(1)–C(15)	1.2998(18)
N(1)–C(16)	1.4113(17)
N(1)–H(1)	0.867(18)
N(2)–C(17)	1.3792(19)
N(2)–H(2)	0.90(2)
N(2)–H(3)	0.94(2)
C(1)–C(2)	1.4148(18)
C(2)–C(3)	1.3859(18)
C(3)–C(4)	1.4136(19)
C(4)–C(5)	1.3721(19)
C(5)–C(6)	1.4373(18)
C(1)–C(6)	1.4187(18)
C(6)–C(15)	1.4176(19)
Angle	**ω, deg**
O(1)Sb(1)O(2)	76.82(3)
O(2)Sb(1)C(28)	163.90(4)
C(34)Sb(1)C(28)	105.56(5)
C(34)Sb(1)O(1)	162.84(5)
O(1S)Sb(1)C(22)	169.62(5)
O(1S)Sb(1)O(2)	87.66(4)
O(1S)Sb(1)C(34)	89.34(5)
O(2)Sb(1)C(34)	89.30(4)
O(1S)Sb(1)C(28)	86.37(5)
O(1S)Sb(1)O(1)	80.18(4)
C(28)Sb(1)O(1)	87.43(4)
O(2)Sb(1)C(22)	86.40(5)
C(34)Sb(1)C(22)	99.08(5)
C(28)Sb(1)C(22)	97.09(5)
O(1)Sb(1)C(22)	90.18(5)

The cationic complex formed undergoes decomposition with the elimination of the *o*-quinone ligand. In dichloromethane the oxidation peaks (Ep^{ox3}, Ep^{ox4}) shifted to the anodic range correspond to the further redox transformations of the organic ligand. The two-electron anodic peak at 1.67 V presumably characterizes the oxidation of the unsubstituted phenol fragment [42]. No electrochemical activity was detected in a more positive range of potential sweep because of the low solubility of complex **IV** in acetonitrile.

Complex **III** containing the aniline group differs in the electrochemical behavior from compound **IV**. The solvent nature significantly affects the oxidation potentials, and the electrochemical parameters undergo changes in the media studied. Four redox steps are detected in dichloromethane for complex **III** at the initial time moment (Fig. 4, 0 min) as in the case of compound **IV**. The replacement of the phenol group by the aniline group affects the potential of the first oxidation step, which is shifted to the cathodic range by 0.08 V.

Changes in the CV curves are observed with time. In particular, the intensity of the peak currents at 0.83 and 1.10 V decreases. The maximum changes are observed for the first irreversible redox transition, the current of which decreases in time against the background of the appearance of the earlier anodic peak at 0.61 V. A regular increase in the anodic peak current (0.61 V) is accompanied by a decrease in the current of the primary peak. The redox transitions appeared in the CV curve is already quasi-reversible (Fig. 4, 13 min). An insignificant shift of the oxidation potential to the anodic range to 1.06 V is also detected for the second anodic process.

Similar changes occurs much more rapidly in acetonitrile (Fig. 5): the initial irreversible oxidation peak at 0.71 V disappears within 4 min (Fig. 5, *1*), and the quasi-reversible redox transition appears at a half-wave potential of 0.51 V. The potential of the second cathodic peak is also shifted from 1.03 to 0.98 V. The color of the solution is from dark cherry in dichloromethane and yellow-red in acetonitrile.

We have earlier observed the significant shift of the oxidation potential of the first redox transition (catecholate/*o*-semiquinolate) for the triphenylantimony(V) 3,6-di-*tert*-butylcatecholate complex in acetonitrile upon the introduction of tetraalkylammonium salts into the solution (Table 3). The coordination of halide anions at the antimony atom results in the formation of the monoanionic hexacoordinated complexes [11]. The negatively charged complex anions are oxidized at the potential shifted to the cathodic range by 0.2–0.3 V. The oxidation potentials of the antimony catecholate complex $[Ph_4Sb][Ph_2Sb(4,5\text{-Cat})_2]$ (4,5-Cat is 4,5-(1,1,4,4-tetramethylbutane-1,4-diyl)catecholate) are also shifted to the cathodic values (0.49, 0.97 V) [35].

The changes in the peak shapes and potentials observed in the CV curves (Figs. 4, 5) can be explained by the proton transfer in a solution from pyrocatechol hydroxyl to the aniline group, which is more basic than the iminomethyl group, to form the catecholate metallocycle (Scheme 4).

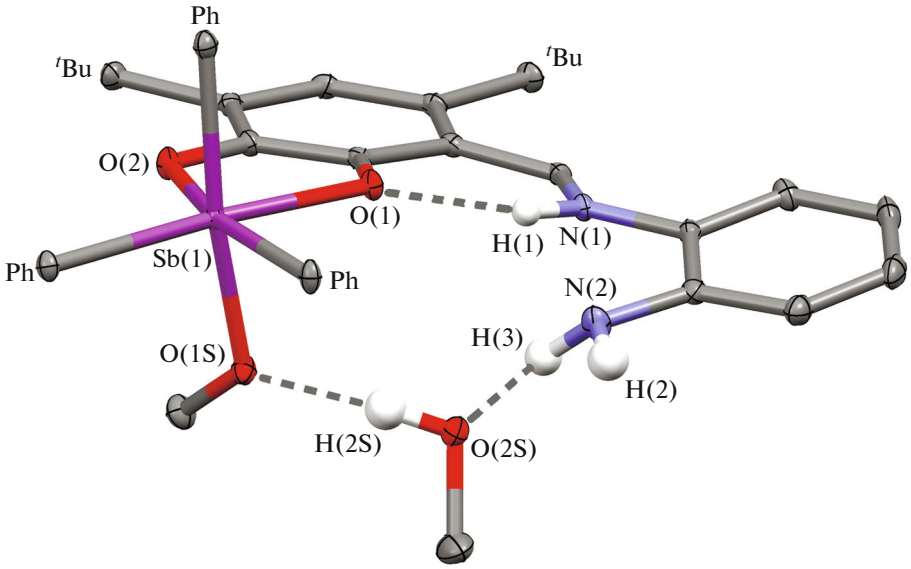

Fig. 2. Molecular structure in the crystal of **III · CH$_3$OH** with the indication of the intramolecular hydrogen bond and intermolecular hydrogen bonds with the solvation methanol molecule.

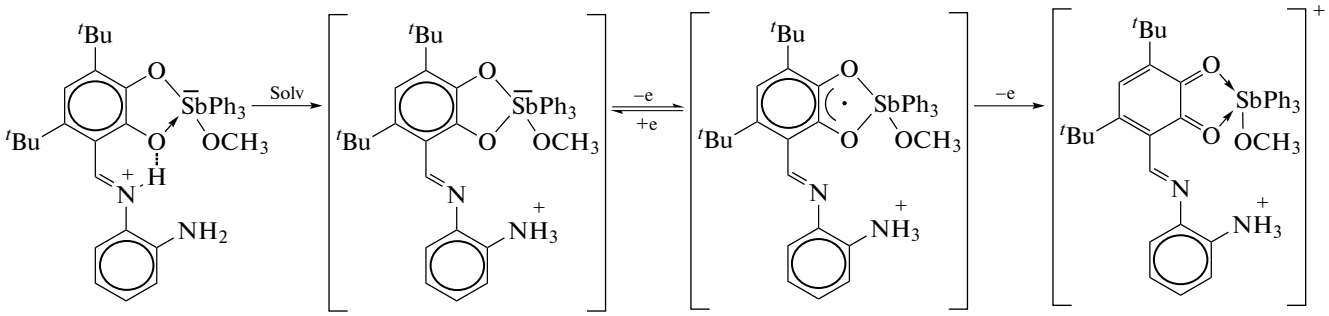

Scheme 4.

As a result, the transformation of complex **III** into **III'** occurring in time is detected in the CV curves in less polar dichloromethane. The reaction occurs much more rapidly in acetonitrile, leading to the detection of

Table 3. Oxidation potentials of the antimony(V) complexes according to the CV data*

Compound	E_p^{ox1}, V**	E_p^{ox2}, V	E_p^{ox3}, V	E_p^{ox4}, V	Solvent
III	0.83	1.10	1.34	1.42	CH_2Cl_2
	0.51***	0.98	1.22	1.34	CH_3CN
IV	0.91	1.25	1.31*	1.67	CH_2Cl_2
	0.91	1.23			CH_3CN
(3,6-Cat)$SbPh_3$****	0.77***	1.29			CH_3CN
[(3,6-Cat)$SbPh_3Br$]NEt_4****	0.56***	0.80			CH_3CN

* GC electrode, $V = 0.2$ V/s, 0.1 M NBu_4ClO_4, $c = 2 \times 10^{-3}$ mol/L, Ar, vs. Ag/AgCl/KCl (sat.).

** E_p^{ox1} is the potential of the irreversible oxidation peak.

*** Half-wave potential for the quasi-reversible anodic process.

**** Published data [11].

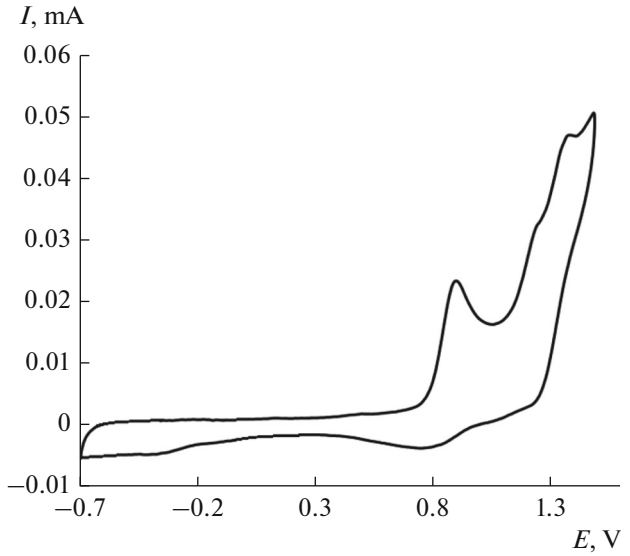

Fig. 3. CV curve for the oxidation of complex **IV** at the potential sweep from –0.70 to 1.50 V (CH_2Cl_2, GC anode, Ag/AgCl/KCl, 0.1 M NBu_4ClO_4, $c = 2 \times 10^{-3}$ mol/L, argon).

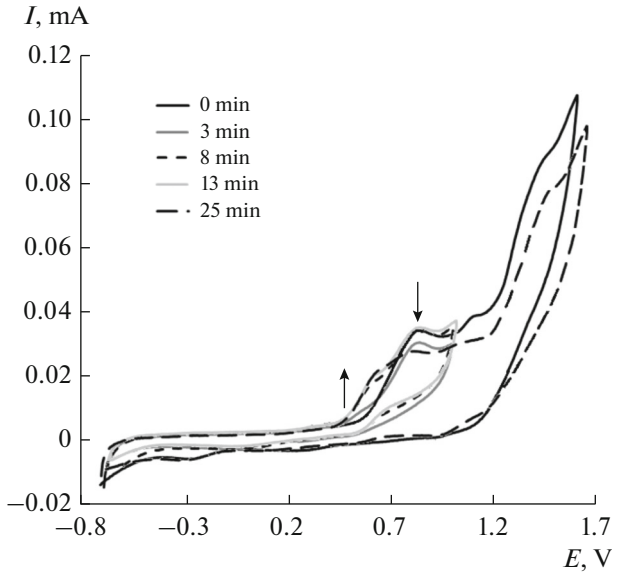

Fig. 4. CV curves for the oxidation of complex **III**: 0 (V = –0.70 to 1.65); 3, 8, and 13 (V = –0.70 to 1.00); 25 min (V = –0.70 to 1.70 V) (CH_2Cl_2, GC anode, Ag/AgCl/KCl, 0.1 M NBu_4ClO_4, $c = 3 \times 10^{-3}$ mol/L, argon).

the electrochemical parameters corresponding to the redox transformations of complex **III'**. The quasi-reversible character of the first anodic peak and the potential values confirm that the catecholate/*o*-semiquinone redox step occurs. The shift of the second anodic oxidation peak to the cathodic range assumes that the irreversible redox transition *o*-semiquinone/*o*-benzoquinone occurs. The oxidation peaks detected in the anodic range at a more anodic potential, as in the case of compound **IV**, assume further redox transformations of the decoordinated ligands.

To conclude, the new triphenylantimony(V) 3,5-di-*tert*-butylcatecholate complexes containing in position 6 of the catecholate ligand the additional functional group (aniline, phenol) bound to the catecholate ring by the iminomethyl group were synthesized. The redox transformations of the methoxytriphenylantimony(V) catecholate complexes were studied by cyclic voltammetry. The electrochemical behavior of the phenol-containing complex is accompanied by the subsequent chemical steps resulting in the oxidation of the catecholate moiety and its decoordination. Aniline–containing methoxytriphenylantimony(V) catecholate is characterized by the transformations in a solution caused by the proton transfer from the imine nitrogen atom to the amino group of the aniline substituent. The nature of the solvent exerts a significant effect on the completeness of the transformation, which occurs completely in more polar acetonitrile. The formed zwitterion contains the monoanionic fragment with the catecholate metallocycle, whose electrochemical oxidation is quasi-reversible at the potential shifted to the cathodic range compared to the starting compound. The observed quasi-reversible process corresponds to the catecholate/*o*-semiquinone redox transition, and the formed intermediate is lowly stable in the time scale of the CV experiment.

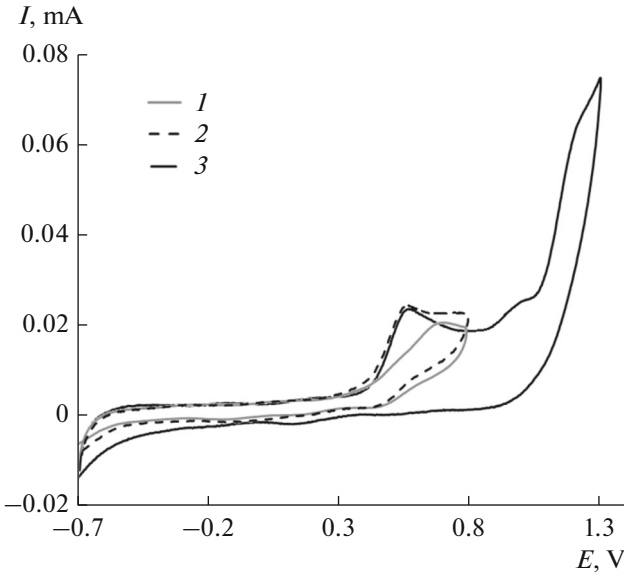

Fig. 5. CV curves for complex **III**: *1*, starting complex (V = –0.70 to 0.80 V); *2*, in 2 min (V = –0.70 to 0.80 V); and *3*, in 4 min (V = –0.70 to 1.40 V) (CH_3CN, GC anode, Ag/AgCl/KCl, 0.1 M NBu_4ClO_4, $c = 2 \times 10^{-3}$ mol/L, argon).

ACKNOWLEDGMENTS

This work was supported by the Russian Foundation for Basic Research, project no. 16-33-60157 mol_a_dk. I.V. Smolyaninov is grateful to the Council for Grants of the President of the Russian Federation for support of the electrochemical studies (project for state support of young Russian scientists, MK-5285.2016.3).

REFERENCES

1. Levason, W. and Reid, G., *Comprehensive Coordination Chemistry II*, Elsevier, 2003, vol. 3, p. 465.
2. Reglinski, J., *Chemistry of Arsenic, Antimony, and Bismuth*, London: Blackie Academic & Professional, 1998.
3. O'Brien, P. and Pickett, N.L., *Comprehensive Coordination Chemistry II*, Elsevier, 2003, vol. 9, p. 1005.
4. Farrell, N., *Comprehensive Coordination Chemistry II*, Elsevier, 2003, vol. 9, p. 809.
5. *Antimony: Characteristics, Compounds and Applications*, Razeghi, M., Ed., New York: Nova Science, 2012.
6. Poddel'sky, A.I., *Antimony: Characteristics, Compounds and Applications*, Razeghi M., Ed., New York: Nova Science, 2012.
7. Poddel'sky, A.I., Baranov, E.V., Fukin, G.K., et al., *J. Organomet. Chem.*, 2013, vol. 733, p. 44.
8. Fukin, G.K., Zakharov, L.N., Domrachev, G.A., et al., *Russ. Chem. Bull.*, 1999, vol. 48, no. 9, p. 1722.
9. Jones, J.S., Wade, C.R., and Gabbai, F.P., *Angew. Chem., Int. Ed. Engl.*, 2014, vol. 53, p. 8876.
10. Tofan, D. and Gabbai, F.P., *Chem. Sci.*, 2016, vol. 7, p. 6768.
11. Poddel'sky, A.I., Ilyakina, E.V., Smolyaninov, I.V., et al., *Russ. Chem. Bull., Int. Ed.*, 2014, vol. 63, no. 4, p. 923.
12. Kuropatov, V.A., Klementieva, S.V., Poddel'sky, A.I., et al., *Russ. Chem. Bull., Int. Ed.,* 2010, vol. 59, no. 9, p. 1698.
13. Abakumov, G.A., Poddel'sky, A.I., Grunova, E.V., et al., *Angew. Chem., Int. Ed. Engl.*, 2005, vol. 44, p. 2767.
14. Poddel'sky, A.I., Kurskii, Yu.A., Piskunov, A.V., et al., *Appl. Organomet. Chem.*, 2011, vol. 25, no. 3, p. 180.
15. Fukin, G.K., Baranov, E.V., Poddel'sky, A.I., et al., *ChemPhysChem*, 2012, vol. 13, no. 17, p. 3773.
16. Poddel'sky, A.I., Smolyaninov, I.V., Kurskii, Yu.A., et al., *Russ. Chem. Bull., Int. Ed.*, 2009, vol. 58, no. 3, p. 532.
17. Poddel'sky, A.I. and Smolyaninov, I.V., *Russ. J. Gen. Chem.*, 2010, vol. 80, no. 3, p. 538.
18. Poddel'sky, A.I., Smolyaninov, I.V., Vavilina, N.N., et al., *Russ. J. Coord. Chem.*, 2012, vol. 38, no. 4, p. 284.
19. Smolyaninov, I.V., Poddel'skii, A.I., Berberova, N.T., et al., *Russ. J. Coord. Chem.*, 2010, vol. 36, no. 9, p. 644.
20. Smolyaninov, I.V., Antonova, N.A., and Poddel'sky, A.I., et al., *J. Organomet. Chem.*, 2011, vol. 696, no. 13, p. 2611.
21. Smolyaninov, I.V., Antonova, N.A., Poddel'sky, A.I., et al., *Dokl. Chem.*, 2012, vol. 443, no. 1, p. 72.
22. Smolyaninov, I.V., Antonova, N.A., Poddel'sky, A.I., et al., *Appl. Organomet. Chem.*, 2012, vol. 26, no. 6, p. 277.
23. Smolyaninov, I.V., Poddel'sky, A.I., Antonova, N.A., et al., *Russ. J. Coord. Chem.*, 2013, vol. 39, no. 2, p. 165.
24. Smolyaninov, I.V., Antonova, N.A., Poddel'sky, A.I., et al., *Appl. Organomet. Chem.*, 2014, vol. 28, p. 274.
25. Smolyaninova, S.A., Poddel'sky, A.I., Smolyaninov, I.V., et al., *Russ. J. Coord. Chem.*, 2014, vol. 40, no. 5, p. 273.
26. Smolyaninov, I.V., Poddel'skii, A.I., Smolyaninova, S.A., et al., *Russ. Chem. Bull., Int. Ed.*, 2015, vol. 64, no. 9, p. 2223.
27. Arsenyev, M.V., Baranov, E.V., Fedorov, A.Yu., et al., *Mendeleev Commun.*, 2015, vol. 25, p. 312.
28. Arsenyev, M.V., Baranov, E.V., Shurygina, M.P., et al., *Mendeleev Commun.*, 2016, vol. 26, p. 552.
29. Baryshnikova, S.V., Bellan, E.V., Poddel'sky, A.I., et al., *Eur. J. Inorg. Chem.*, 2016, p. 5230.
30. Gordon, A. and Ford, R., *The Chemist's Companion: A Handbook of Practical Data, Techniques, and References*, New York: Wiley, 1972.
31. Arsenyev, M.V., Baranov, E.V., Chesnokov, S.A., et al., *Russ. Chem. Bull., Int. Ed.*, 2013, vol. 62, no. 11, p. 2394.
32. Sheldrick, G.M. *SHELXTL. Version 6.14. Structure Determination Software Suite*, Madison: Bruker AXS, 2003.
33. Sheldrick, G.M., *SADABS. Version 2012/1. Bruker/Siemens Area Detector Absorption Correction Program*, Madison: Bruker AXS, 2012.
34. Cherkasov, V.K., Abakumov, G.A., Grunova, E.V., et al., *Chem.-Eur. J.*, 2006, vol. 12, no. 14, p. 3916.
35. Poddel'sky, A.I., Smolyaninov, I.V., Somov, N.V., et al., *J. Organomet. Chem.*, 2010, vol. 695, no. 4, p. 530.
36. Poddel'sky, A.I., Smolyaninov, I.V., Berberova, N.T., et al., *J. Organomet. Chem.*, 2015, vol. 789–790, p. 8.
37. Poddel'sky, A.I., Smolyaninov, I.V., Fukin, G.K., et al., *J. Organomet. Chem.*, 2016, vol. 824, p. 1.
38. Poddel'sky, A.I., Druzhkov, N.O., Fukin, G.K., et al., *Polyhedron*, 2017, vol. 124, p. 41.
39. Poddel'sky, A.I., Arsenyev, M.V., Astaf'eva, T.V., et al., *J. Organomet. Chem.*, 2017, vol. 835, p. 17.
40. Poddel'sky, A.I., Smolyaninov, I.V., Kurskii, Yu.A., et al., *J. Organomet. Chem.*, 2010, vol. 695, no. 8, p. 1215.
41. Batsanov, S.S., *Zh. Neorg. Khim.*, 1991, vol. 36, no. 12, p. 3015.
42. Lund, H. and Hammerich, O., *Organic Electrochemistry*, New York: Marcel Dekker Inc., 2001.

Translated by E. Yablonskaya